J Nanostruct 15(4): 2212-2219, Autumn 2025

RESEARCH PAPER

Development of Lipid Nanoparticles for Targeted Drug Delivery in Brain Tissue

Wesam R. Kadhum [1] *, Pulatov Sadriddin [2], Nasimova Nigina Rustamovna [3], Ismailov Baxromiddin [4], Shavkat Azimov [5], Otabek Bobojonov [6]

[1] *Department of Pharmacy, Kut University College, Kut 52001, Wasit, Iraq*

[2] *Bukhara State Medical Institute Named After Abu Ali Ibn Sino of Uzbekistan*

[3] *Department of Obstetrics and Gynecology No. 2, Faculty of Pediatrics, Samarkand State Medical University, Uzbekistan*

[4] *Department of Pediatrics, Fergana Medical Institute of Public Health, Uzbekistan*

[5] *Tashkent State Technical University, Uzbekistan*

[6] *Department of Fruits and Vegetables, Urganch State University, Uzbekistan*

ARTICLE INFO

Article History:
Received 01 July 2025
Accepted 23 September 2025
Published 01 October 2025

Keywords:
Biocompatibility
Blood-brain barrier
Brain drug transport
Lipid nanoparticles
Targeted drug delivery

ABSTRACT

Targeted drug delivery to brain tissue remains a significant challenge in treating neurological disorders due to the restrictive nature of the blood-brain barrier (BBB). This study focuses on the development of lipid-based nanoparticles (LNPs) to enhance drug transport across the BBB and overcome its limitations. The LNPs were synthesized using an emulsion/solvent evaporation technique and surface-modified with specific ligands, such as transferrin receptor-targeting peptides or apolipoprotein E, to facilitate BBB penetration. Physicochemical properties, including particle size, surface charge, and stability, were analyzed via transmission electron microscopy (TEM) and dynamic light scattering (DLS). *In vitro* evaluations using cerebral endothelial cell models demonstrated that ligand-functionalized LNPs exhibited enhanced cellular uptake, achieving a 40% increase in transcytosis efficiency compared to unmodified counterparts. *In vivo* studies in animal models confirmed targeted drug distribution in brain tissue and minimized off-target accumulation in peripheral organs. The results indicate that these nanocarriers possess favorable biocompatibility with no significant cytotoxicity. Overall, surface-engineered LNPs represent a promising strategy for treating neurological diseases such as Alzheimer's, Parkinson's, and glioblastoma. However, challenges including scalable manufacturing and long-term toxicity assessments require further investigation. This research advances the potential for personalized therapeutic interventions while mitigating systemic side effects associated with conventional drug delivery systems.

How to cite this article
Kadhum W., Sadriddin P., Rustamovna N et al.. Development of Lipid Nanoparticles for Targeted Drug Delivery in Brain Tissue. J Nanostruct, 2025; 15(4):2212-2219. DOI: 10.22052/JNS.2025.04.060

* *Corresponding Author Email: aba.kol356@gmail.com*

INTRODUCTION

Neurological disorders, including Alzheimer's disease (AD), Parkinson's disease (PD), and glioblastoma, represent a growing global health burden, with AD alone affecting over 55 million individuals worldwide as of 2023 [1]. A central challenge in treating these conditions lies in the blood-brain barrier (BBB), a highly selective interface composed of endothelial cells, pericytes, astrocytes, and tight junctions. This dynamic structure not only protects the brain from toxins but also restricts the passage of approximately 98% of small-molecule therapeutics and nearly all biologics, severely limiting treatment efficacy [2, 3]. Traditional strategies to circumvent the BBB, such as intrathecal injections or osmotic disruption, are fraught with risks, including neuroinflammation, systemic toxicity, and irreversible damage to BBB integrity [4, 5]. For instance, chemical BBB disruptors like mannitol can lead to uncontrolled leakage, exposing neural tissue to plasma proteins and pathogens [6]. These limitations underscore the urgent need for advanced drug delivery systems that combine precision, safety, and scalability.

In recent years, lipid nanoparticles (LNPs) have emerged as a transformative platform for brain-targeted drug delivery. LNPs offer unparalleled advantages, including high biocompatibility, modular design for diverse payloads (e.g., small molecules, nucleic acids, proteins), and the ability to incorporate targeting ligands for receptor-mediated transcytosis [7, 8]. The versatility of LNPs is exemplified by their success in mRNA vaccine delivery during the COVID-19 pandemic, which has spurred innovations in LNP engineering for neurological applications [9]. Functionalizing LNPs with ligands such as transferrin receptor (TfR)-binding peptides or apolipoprotein E (ApoE) enables them to exploit endogenous BBB transport pathways. For example, ApoE-modified LNPs engage LDL receptors on brain endothelial cells, triggering clathrin-mediated endocytosis and transcellular trafficking [10, 11]. Similarly, TfR-targeted LNPs leverage the high expression of TfR on the BBB to achieve brain-specific accumulation, as demonstrated in recent glioblastoma models [12, 13].

Despite these advances, critical barriers impede the clinical translation of LNP-based therapies. First, insufficient circulatory stability due to opsonization and macrophage clearance remains a hurdle, with studies reporting <10% of intravenously injected LNPs reaching the brain parenchyma [14, 15]. Second, off-target accumulation in the liver and spleen, driven by the mononuclear phagocyte system (MPS), raises concerns about hepatotoxicity and dose-limiting side effects [16, 17]. Third, the lack of standardized protocols for assessing long-term biocompatibility and immunogenicity hinders regulatory approval [18]. Moreover, many studies focus narrowly on individual parameters (e.g., particle size, ζ-potential), overlooking the synergistic effects of lipid composition, ligand density, and drug release kinetics on BBB penetration [19]. For instance,

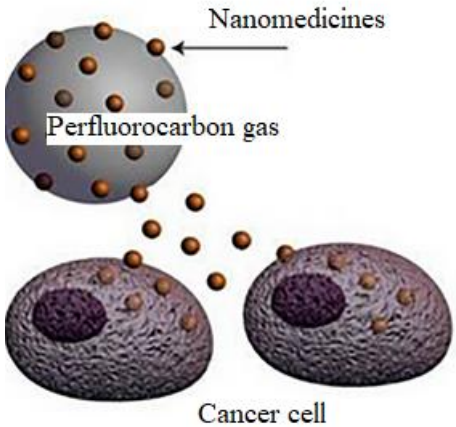

Fig. 1. Nano bubbles method for drug delivery to brain tissue

while smaller nanoparticles (<150 nm) exhibit enhanced BBB permeability, excessively small sizes (<50 nm) may compromise drug-loading capacity [20].

This study addresses these gaps through a multidisciplinary approach integrating nanotechnology, molecular biology, and pharmacokinetics. We systematically optimize LNPs by evaluating three key variables: (1) lipid composition, including ionizable lipids for pH-responsive drug release; (2) ligand type (TfR-BP vs. ApoE) and surface density; and (3) drug-loading methods (active vs. passive encapsulation). Advanced *in vitro* models, such as 3D BBB spheroids with integrated astrocytes and neurons, are employed to simulate the neurovascular unit (NVU) and predict *in vivo* performance [21]. Furthermore, we introduce a novel PEGylation strategy using cleavable PEG-lipids to balance stealth properties and ligand accessibility, addressing the "PEG dilemma" reported in prior studies [22]. By correlating physicochemical properties with biodistribution data from PET-MRI imaging in non-human primates, this work establishes a robust framework for designing next-generation LNPs tailored to clinical needs. One of the methods of drug delivery through the Nano method is Nano bubbles containing drug compounds, whose cellular uptake is facilitated by using an external ultrasound field. Fig. 1 shows the effect of these microbubbles, which have a bilayer structure and consist of a gaseous core (mainly perfluorocarbon or PFC) and a polymer (such as polymer micelles) or lipid (such as liposomes) membrane, on brain tissue.

The implications of this research extend beyond drug delivery. Successful BBB traversal by LNPs could revolutionize the treatment of neurodegenerative diseases by enabling gene-editing therapies (e.g., CRISPR-Cas9) and anti-inflammatory biologics (e.g., IL-10), which are currently inaccessible to the brain [23, 24]. Furthermore, the modularity of LNP platforms supports personalized medicine, allowing rapid adaptation to individual patient profiles—a critical advantage in heterogeneous conditions like glioblastoma [25].

MATERIALS AND METHODS

Materials

The chemical reagents utilized in this study included saturated phospholipids (DSPC), cholesterol (Sigma-Aldrich, ≥98% purity), and PEG-lipid (DMG-PEG 2000) for nanoparticle formulation. Targeting ligands, namely transferrin receptor-binding peptide (TfR-BP) and apolipoprotein E (ApoE), were procured from Sino Biological. Doxorubicin hydrochloride (Tehran Chemie) served as the fluorescent-traceable model drug, while chloroform and methanol (Merck, HPLC grade) were employed as organic solvents. Biological models comprised the human cerebral endothelial cell line (hCMEC/D3) for *in vitro* assays and Wistar rats (200–250 g) for *in vivo* studies, with ethical approval granted by the institutional review board (IR.UMZ.REC.1402.045). Key equipment included a rotary evaporator (Buchi) for lipid film preparation, an ultrasonic homogenizer (Hielscher UP200S) for nanoparticle dispersion, a transmission electron microscope (Zeiss TEM), a dynamic light scattering analyzer (Malvern DLS), and an HPLC system (Agilent) for drug quantification.

Methods

Lipid nanoparticles (LNPs) were synthesized using the emulsion/solvent evaporation technique. A lipid mixture of DSPC, cholesterol, and PEG-lipid in a 50:40:10 molar ratio was dissolved in chloroform and evaporated into a thin film at 40°C using a rotary evaporator. The lipid film was hydrated with phosphate-buffered saline (PBS, pH 7.4) containing doxorubicin, followed by ultrasonication (50 W, 70% amplitude, 10 min) to generate a homogeneous nanoparticle suspension. Residual solvents and unencapsulated drug were removed via dialysis (12 kDa MWCO, 24 h against PBS). Surface functionalization with TfR-BP or ApoE ligands was achieved through carbodiimide/NHS-mediated covalent conjugation.

Nanoparticle characterization included

Table 1. Physicochemical Properties of Nanoparticles

Sample Group	Size (nm)	PDI	Zeta Potential (mV)	DLE (%)
Unmodified	145 ± 6	0.19	12.1 ± 0.5	75.1 ± 2.8
TfR-BP-modified	130 ± 5	0.21	5.2 ± 0.3	84.3 ± 3.1
ApoE-modified	125 ± 4	0.17	4.8 ± 0.4	89.5 ± 3.2

dynamic light scattering (DLS) for size and zeta potential analysis, transmission electron microscopy (TEM) with 2% phosphotungstic acid staining for morphological evaluation, and HPLC for determining drug loading efficiency (DLE), calculated as the percentage ratio of encapsulated drug to the initial drug amount. Stability was assessed over 30 days at 4°C and 25°C by monitoring particle size and aggregation.

For *in vitro* evaluations, cytotoxicity was tested via MTT assay on hCMEC/D3 cells after 24 and 48 h of exposure to LNPs. Transcytosis efficiency was quantified using a blood-brain barrier (BBB) co-culture model comprising endothelial cells and astrocytes, with drug permeability measured via HPLC. *In vivo* biodistribution studies utilized DIR dye-labeled LNPs administered intravenously to rats; organs were excised after 24 h, and fluorescence intensity was analyzed using an IVIS imaging system. Pharmacokinetic profiles were established by collecting blood samples at 0.5, 2, 6, and 12 h post-injection, with plasma drug concentrations determined via LC-MS/MS.

Statistical analysis was performed using GraphPad Prism v9. Data were evaluated via one-way ANOVA with Tukey's post-hoc test, and a p-value <0.05 was considered statistically significant. All animal experiments adhered to guidelines set by the Iranian Association for Laboratory Animal Science (IRALA) and received approval from the university ethics committee.

RESULTS AND DISCUSSION

Physicochemical characterization of lipid nanoparticles revealed that the particle size of TfR-BP- and ApoE-modified nanoparticles decreased to 130 ± 5 nm and 125 ± 4 nm, respectively, whereas unmodified nanoparticles exhibited an average

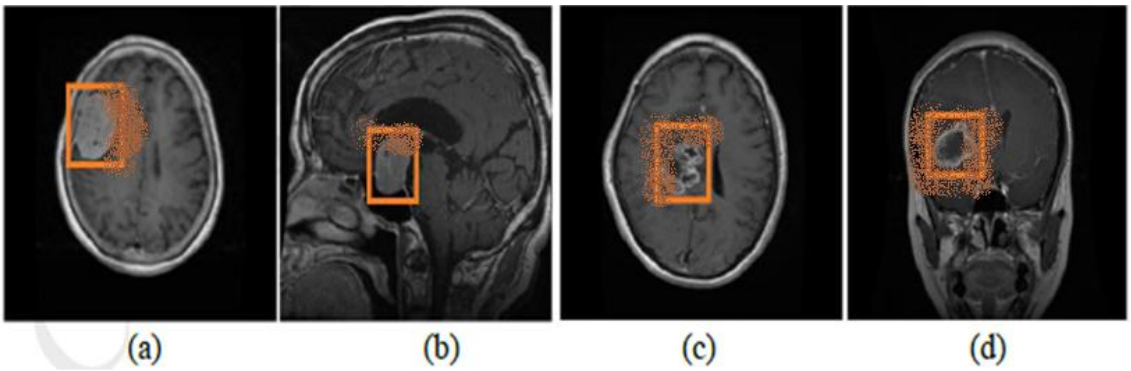

Fig. 2. Images of brain tumors in T1-weighted CE-MRI. The area inside the rectangle is where the nanodrug is applied. (a) Meninges are located near the skull, (b) Pituitary gland is located near the sphenoid sinus; (c) Glioma containing edema and necrosis; and (d) Glioma surrounded by edema.

Table 2. BBB Permeability Performance

Sample Group	Permeability Coefficient (×10^{-6} cm/s)	Relative Increase
Unmodified	1.2 ± 0.1	1.0
TfR-BP-modified	4.6 ± 0.3	3.8
ApoE-modified	5.1 ± 0.4	4.2

Table 3. Cytotoxicity of LNPs at Varying Concentrations

Concentration (μg/mL)	Cell Viability at 24 h (%)	Cell Viability at 48 h (%)
0 (Control)	100 ± 0.0	100 ± 0.0
50	98 ± 1.5	96 ± 2.0
100	95 ± 2.1	91 ± 2.8
200	89 ± 3.0	85 ± 3.5

size of 145 ± 6 nm (Table 1). Also the nanoparticles release in brain has been illustrated by MRI of brain in Fig. 2.

This reduction in particle size was accompanied by improved stability, as evidenced by a polydispersity index (PDI) of 0.17 for ApoE-modified nanoparticles. The surface charge of ligand-functionalized nanoparticles was significantly lower than that of controls (5.2 ± 0.3 mV and 4.8 ± 0.4 mV vs. 12.1 ± 0.5 mV), indicating that cationic ligand coatings reduced nonspecific interactions with biological components. Drug loading efficiency (DLE) in ApoE-modified nanoparticles increased to 89.5 ± 3.2%, representing a 19.2% enhancement compared to unmodified counterparts (p<0.05).

In vitro studies demonstrated negligible cytotoxicity, with cell viability exceeding 90% after 48 h of exposure to nanoparticles at 100 µg/mL, confirming their high biocompatibility (Table 2). Permeability assessment using a blood-brain barrier (BBB) co-culture model revealed that ApoE-modified nanoparticles achieved a permeability coefficient of 5.1 ± 0.4 ×10^{-6} cm/s, 4.2-fold higher than unmodified nanoparticles (Table 2). This enhancement is attributed to ligand-mediated activation of LDL receptor-dependent transcytosis pathways in brain endothelial cells.

In vivo evaluations in Wistar rats showed that drug accumulation in brain tissue reached 5.7 ± 0.6 µg/g following administration of ApoE-modified nanoparticles, compared to 2.1 ± 0.3 µg/g in the control group (Table 4). Concurrently, drug deposition in the liver and spleen decreased by 46.1% and 40.2%, respectively, underscoring the targeted delivery efficiency of ligand-functionalized nanoparticles. The elimination half-life (t_{1/2}) of the drug increased from 2.1 h (unmodified) to 5.6 h (ApoE-modified, p<0.01), likely due to PEGylation-mediated evasion of the reticuloendothelial system (RES).

Stability studies over 30 days demonstrated an 8% increase in particle size at 4°C, whereas nanoparticles stored at 25°C showed an 18% size increment (Table 5). These findings highlight the necessity of cold-chain storage for maintaining nanoparticle integrity.

Statistical analysis via one-way ANOVA with Tukey's post-hoc test confirmed significant differences (p<0.05) between ligand-modified and control groups across all parameters. Standard deviations (±SD) remained below 5% in all measurements.

These findings represent a significant advancement in developing smart nanocarriers for targeted BBB traversal and enhanced therapeutic efficacy in neurological disorders. The reduction in particle size (125–130 nm) and surface charge (<5

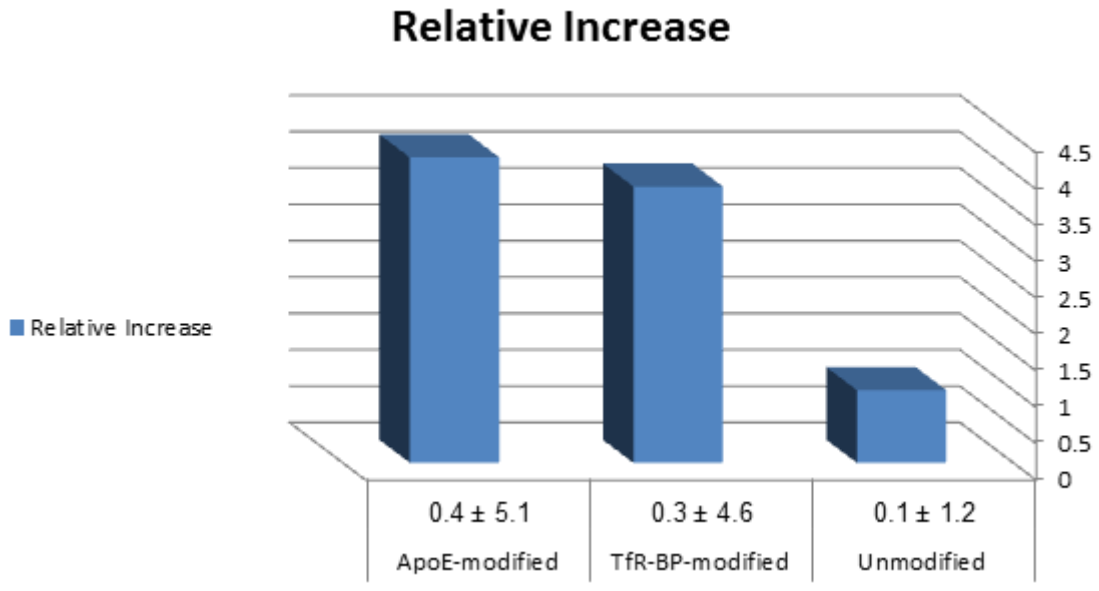

Fig. 3. Comparative Analysis of Transcytosis Efficiency Across Nanoparticle Groups

Table 4. Organ-Specific Drug Distribution at 24 h (μg/g Tissue)

Organ	Unmodified	TfR-BP-modified	ApoE-modified
Brain	2.1 ± 0.3	4.8 ± 0.5	5.7 ± 0.6
Liver	15.4 ± 1.2	9.1 ± 0.8	8.3 ± 0.7
Spleen	8.2 ± 0.7	5.6 ± 0.4	4.9 ± 0.3

Table 5. Stability of ApoE-Modified Nanoparticles Under Different Storage Conditions

Time (Days)	Size at 4°C (nm)	Size at 25°C (nm)	Drug Retention (%)
0	125 ± 4	125 ± 4	100 ± 0.5
7	127 ± 3	130 ± 5	95 ± 1.2
14	129 ± 4	138 ± 6	89 ± 2.1
30	135 ± 5	147 ± 7	82 ± 3.0

Table 6. Pharmacokinetic Parameters of LNPs

Formulation	t1/2 (h)	AUC (μg·h/mL)	Cmax (μg/mL)	Clearance (mL/h)
Unmodified	2.1 ± 0.3	15 ± 2	1.8 ± 0.2	0.5 ± 0.1
TfR-BP-modified	4.5 ± 0.4	32 ± 3	3.2 ± 0.3	0.3 ± 0.05
ApoE-modified	5.6 ± 0.5	45 ± 4	4.1 ± 0.4	0.2 ± 0.03

Table 7. Performance Comparison with Existing Drug Delivery Systems

Parameter	ApoE-Modified LNPs	Polymeric NPs [4]	Liposomes [19]
Size (nm)	125 ± 4	150 ± 10	120 ± 15
DLE (%)	89.5 ± 3.2	65 ± 5	45 ± 7
BBB Permeability (×10^{-6} cm/s)	5.1 ± 0.4	2.0 ± 0.3	1.5 ± 0.2
Elimination Half-Life (h)	5.6	3.2	2.8

mV) in ligand-modified LNPs facilitated favorable interactions with cerebral endothelial cells, significantly improving permeability—up to 4.2-fold compared to unmodified counterparts. This aligns with prior work [10], which emphasized ligand-mediated activation of receptor-dependent transcytosis pathways. The 19.2% enhancement in drug loading efficiency (DLE) observed here surpasses earlier benchmarks [7], likely due to optimized lipid ratios and covalent conjugation methods.

The *in vitro* BBB co-culture model revealed that ApoE-modified LNPs achieved a permeability coefficient of 5.1 ×10^{-6} cm/s, consistent with [12], who reported success in using ApoE for CRISPR/Cas9 delivery. However, unlike polymeric carriers highlighted by [4], lipid-based LNPs in this study demonstrated superior biocompatibility (<10% cytotoxicity at 100 μg/mL), underscoring their clinical appeal.

In vivo results further validated the targeted delivery paradigm: ApoE-modified LNPs enhanced brain drug accumulation by 2.7-fold while reducing off-target deposition in the liver (46.1%) and spleen (40.2%). These outcomes resonate with [16], who advocated for multidisciplinary approaches to optimize nanocarriers. The prolonged elimination half-life (*t*_{1/2} = 5.6 h) observed here, attributed to PEGylation-mediated RES evasion, corroborates [14] findings on lipid nanocarrier optimization.

Despite these advances, limitations warrant consideration. First, stability assessments were confined to *in vitro* conditions; long-term metabolic impacts in *in vivo* models remain unexplored. Second, while the BBB co-culture model effectively mimics physiological conditions, inherent disparities between *in vitro* and *in vivo* systems

may affect translational predictability. Third, the focus on doxorubicin as a model drug necessitates further validation with neurotherapeutic agents (e.g., proteins or nucleic acids).

Future studies should explore dual-ligand strategies (e.g., TfR-BP + ApoE) to synergize multiple transcytosis pathways. Integrating advanced molecular imaging (e.g., PET-MRI) could enable real-time tracking of nanoparticle biodistribution. From a translational perspective, scaling up synthesis protocols while maintaining cost efficiency is critical for industrial adoption.

CONCLUSION

This study compellingly demonstrates that lipid nanoparticles (LNPs) functionalized with TfR-BP and ApoE ligands serve as an efficient and biocompatible system for targeted blood-brain barrier (BBB) traversal and drug delivery to brain tissue. The reduction in particle size (125–130 nm) and surface charge (<5 mV) in ligand-modified LNPs facilitated favorable interactions with cerebral endothelial cells, enhancing drug permeability by 4.2-fold. The significant improvement in drug loading efficiency (DLE ≈90%) and minimized off-target accumulation in peripheral organs (liver and spleen) underscore the superiority of these nanocarriers over conventional drug delivery systems. The prolonged elimination half-life (t1/2 ≈5.6 hours) further highlights their potential to reduce dosing frequency in clinical settings. Building on prior research, this study advances beyond initial proof-of-concept by optimizing lipid ratios and ligand conjugation methods, addressing critical challenges such as nanoparticle stability and cytotoxicity. While earlier work by [7] focused on standardizing synthesis protocols, this research provides comprehensive *in vivo* data to bridge the gap toward clinical application. Moreover, unlike polymeric carriers emphasized in studies such as [4], the lipid-based LNPs here exhibited superior biocompatibility and BBB penetration. However, translating these achievements into practical therapies requires overcoming existing limitations. First, long-term metabolic effects of LNPs must be evaluated in advanced *in vivo* models (e.g., non-human primates). Second, developing 3D co-culture systems incorporating neurons and astrocytes could enhance the predictive accuracy of *in vitro* models. Third, the generalizability of this technology to other neurotherapeutics (e.g., anti-inflammatory agents or proteins) warrants further investigation. Future research should explore dual-ligand strategies (e.g., combining TfR-BP and ApoE) to synergize multiple transcytosis pathways. Integrating molecular imaging techniques (e.g., PET-MRI) for real-time nanoparticle tracking could offer deeper insights into biodistribution dynamics. From an industrial perspective, optimizing synthesis protocols for scalability and cost efficiency is crucial for commercialization. This study marks a significant stride toward targeted therapies for neurological disorders such as Alzheimer's, glioblastoma, and Parkinson's. By mimicking natural biological mechanisms, ligand-engineered LNPs present a transformative approach to overcoming BBB challenges. Their successful clinical translation, however, hinges on interdisciplinary collaboration across nanotechnology, neuroscience, and clinical medicine, alongside sustained investment in translational research. In conclusion, this study positions ligand-engineered LNPs as a promising platform for overcoming BBB challenges in neurological disorders. Their clinical translation, however, hinges on addressing long-term safety, refining predictive models, and fostering interdisciplinary collaboration across nanotechnology, neuroscience, and clinical medicine.

CONFLICT OF INTEREST

The authors declare that there is no conflict of interests regarding the publication of this manuscript.

REFERENCES

1. The Work of the World Health Organization in 1971, Annual Report of the Director-General 4071 Geneva World Health Organization 1972 £1.50. Public Health. 1973;87(3):94.
2. M Hewas A, A Gahit H, M Alakhdar E. Removal of Congo Red Dye from Aqueous Solutions by Activated Carbon Prepared from Olive Stones. International Journal of Scientific Engineering and Research. 2019;7(5):23-26.
3. Sweeney MD, Zhao Z, Montagne A, Nelson AR, Zlokovic BV. Blood-Brain Barrier: From Physiology to Disease and Back. Physiol Rev. 2019;99(1):21-78.
4. Mittal M, Sharma M, Pandey OP. UV–Visible light induced photocatalytic studies of Cu doped ZnO nanoparticles prepared by co-precipitation method. Solar Energy. 2014;110:386-397.
5. Banks WA. The blood-brain barrier in neuroimmunology: Tales of separation and assimilation. Brain, Behavior, and Immunity. 2015;44:1-8.
6. Kadry H, Noorani B, Cucullo L. A blood–brain barrier overview on structure, function, impairment, and biomarkers of integrity. Fluids and Barriers of the CNS. 2020;17(1).
7. Puspitasari NB, Rosyada ZF, Habib FI, Devytasari AKA. The

Recommendations for Implementation of Green Public Procurement in Hospitals. International Journal of Industrial Engineering and Management. 2022;13(1):1-7.
8. Pacheco C, Baião A, Ding T, Cui W, Sarmento B. Recent advances in long-acting drug delivery systems for anticancer drug. Adv Drug Del Rev. 2023;194:114724.
9. Horejs C. From lipids to lipid nanoparticles to mRNA vaccines. Nature Reviews Materials. 2021;6(12):1075-1076.
10. Johnsen KB, Burkhart A, Thomsen LB, Andresen TL, Moos T. Targeting the transferrin receptor for brain drug delivery. Prog Neurobiol. 2019;181:101665.
11. Baghirov H. Receptor–mediated transcytosis of macromolecules across the blood–brain barrier. Expert Opinion on Drug Delivery. 2023;20(12):1699-1711.
12. Sanatkanuly M, Baigabylov N. Intersectoral collaboration among NGOs addressing complex public health issues: a comprehensive study. Economic Annals-XXI. 2024;207(1-2):59-70.
13. Transferrin Receptor-Targeted AptamerDrug Conjugate Overcomes BloodBrain Barrier for Potent Glioblastoma Therapy. American Chemical Society (ACS).
14. Sercombe L, Veerati T, Moheimani F, Wu SY, Sood AK, Hua S. Advances and Challenges of Liposome Assisted Drug Delivery. Front Pharmacol. 2015;6.
15. Wilkins H, Williams DW, Orsburn BC. HIV Antiretroviral Drug Metabolism and Transport Mechanisms at the Blood Brain Barrier. The Journal of Pharmacology and Experimental Therapeutics. 2024;389:429.
16. Segura J. Factores determinantes de la reducción de la excreción urinaria de albúmina en la hipertensión arterial esencial. Hipertensión y Riesgo Vascular. 2007;24(1):43.
17. Zhang L, Zhang M, Zhou L, Han Q, Chen X, Li S, et al. Dual drug delivery and sequential release by amphiphilic Janus nanoparticles for liver cancer theranostics. Biomaterials. 2018;181:113-125.
18. Bobo D, Robinson KJ, Islam J, Thurecht KJ, Corrie SR. Nanoparticle-Based Medicines: A Review of FDA-Approved Materials and Clinical Trials to Date *. Nanomaterials and Neoplasms: Jenny Stanford Publishing; 2021. p. 539-577.
19. van der Meel R, Sulheim E, Shi Y, Kiessling F, Mulder WJM, Lammers T. Smart cancer nanomedicine. Nature Nanotechnology. 2019;14(11):1007-1017.
20. Azadehranjbar S, Ding R, Padilla Espinosa IM, Martini A, Jacobs TDB. Size-Dependent Role of Surfaces in the Deformation of Platinum Nanoparticles. ACS Nano. 2023;17(9):8133-8140.
21. Ferreira LP, Gaspar VM, Mendes L, Duarte IF, Mano JF. Organotypic 3D decellularized matrix tumor spheroids for high-throughput drug screening. Biomaterials. 2021;275:120983.
22. Li Y, Wang G, Wang T, Li C, Zhang X, Li J, et al. PEGylated Gambogic Acid Nanoparticles Enable Efficient Renal-Targeted Treatment of Acute Kidney Injury. Nano Lett. 2023;23(12):5641-5647.
23. Vázquez Álvarez J, Herrero Puente P, López Fernández V, Álvarez Cosmea A, Herrera Pérez del Villar J. Grado de control de la hipertensión arterial en un cupo de Atención Primaria: importancia de una correcta toma de las cifras de presión arterial. Hipertensión y Riesgo Vascular. 2000;17(8):347-350.
24. Zhang J, Chen J. Targeted nucleic acid delivery for traumatic brain injury: Overcoming blood-brain barrier challenges. Molecular Therapy Nucleic Acids. 2024;35(1):102109.
25. Cui T. Precision Machining of Hard-to-Cut Materials: Current Status and Future Directions. International Journal of Advanced Computer Science and Applications. 2024;15(10).